The EMBO Journal vol.15 no.21 pp.5772–5782, 1996

Loss of growth polarity and mislocalization of septa in a *Neurospora* mutant altered in the regulatory subunit of cAMP-dependent protein kinase

Kenneth S.Bruno, Rodolfo Aramayo[1], Peter F.Minke, Robert L.Metzenberg[1] and Michael Plamann[2]

Department of Biology, Texas A&M University, College Station, TX 77843-3258 and [1]Department of Biomolecular Chemistry, University of Wisconsin Medical School, 687 Medical Sciences Building, Madison, WI 53706-1532, USA

[2]Corresponding author

In filamentous fungi, growth polarity (i.e. hyphal extension) and formation of septa require polarized deposition of new cell wall material. To explore this process, we analyzed a conditional *Neurospora crassa* mutant, *mcb*, which showed a complete loss of growth polarity when incubated at the restrictive temperature. Cloning and DNA sequence analysis of the *mcb* gene revealed that it encodes a regulatory subunit of cAMP-dependent protein kinase (PKA). Unexpectedly, the *mcb* mutant still formed septa when grown at the restrictive temperature, indicating that polarized deposition of wall material during septation is a process that is, at least in part, independent of polarized deposition during hyphal tip extension. However, septa formed in the *mcb* mutant growing at the restrictive temperature are mislocalized. Both polarized growth and septation are actin-dependent processes, and a concentration of actin patches is observed at growing hyphal tips and sites where septa are being formed. In the *mcb* mutant growing at the restrictive temperature, actin patches are uniformly distributed over the cell cortex; however, actin patches are still concentrated at sites of septation. Our results suggest that the PKA pathway regulates hyphal growth polarity, possibly through organizing actin patches at the cell cortex.

Keywords: actin/adenylate cyclase/growth polarity/protein kinase A/septation

Introduction

Polarity of cell growth is fundamental to morphogenesis of most, if not all, unicellular and multicellular organisms (Harold, 1990). One of the most extreme examples of growth polarity is found in the filamentous fungi. The basic growth unit of filamentous fungi, the hypha, results from continuous deposition of new cell wall material at a specific site, the hyphal apex. In the ascomycete *Neurospora crassa*, hyphae are typically 4–12 μm in diameter, extend exclusively from tips, and branch at irregular intervals to produce a radially spreading colony (McLean and Prosser, 1987). While the bulk of new cell wall growth occurs at hyphal apices, polarized deposition of wall material also occurs during septation, a process akin to cytokinesis in animal cells (Patton and Marchant, 1978; Girbardt, 1979; Gabriel, 1984). During septation in *N.crassa*, internal cell walls (septa) are laid down and cellularize hyphal filaments into multinucleate compartments.

Ultrastructural studies have revealed that the hyphal apex lacks nuclei and mitochondria, but is rich in cytoplasmic vesicles (Grove and Bracker, 1970). These have been proposed to contain enzymes and precursors necessary for the production of new cell membrane and wall (Gooday, 1971; Gooday and Trinci, 1980). The most studied components of the cytoskeleton of filamentous fungi are actin and microtubules, which are thought to be involved in cytoplasmic migration and organelle movement (McKerracher and Heath, 1987). The majority of filamentous actin is localized to the hyphal tips, and in some fungi it occurs as an apical cap composed of patches and fine filaments (McKerracher and Heath, 1987; Barja *et al.*, 1990; Heath, 1990). Proper actin organization is required for polarized growth at hyphal tips (Grove and Sweigard, 1980), whereas proper microtubule organization is required for tip extension in *N.crassa*, but not for hyphal tip formation (That *et al.*, 1988).

Genetic approaches have been used in the unicellular fungi *Saccharomyces cerevisiae* and *Schizosaccharomyces pombe* to identify genes required for morphogenesis (Chant, 1994; Nurse, 1994; Cid *et al.*, 1995). Among the morphological mutants isolated in *S.cerevisiae* and *S.pombe* are conditional mutants lacking growth polarity at the restrictive temperature (Chant, 1994; Verde *et al.*, 1995). Extensive analysis of genes controlling bud site selection and polarized growth during bud formation has led to elucidation of a molecular pathway for cell polarity in *S.cerevisiae* (Cid *et al.*, 1995; Drubin and Nelson, 1996). Rsr1p, Bud2-5p and Axl1p have been identified as proteins required for selecting the site on the cortex of the mother cell at which the bud will emerge. Cdc42p, a Ras-like GTP binding protein, controls the establishment of a polarized actin cytoskeleton at the site of bud emergence. In *S.cerevisiae*, as in other eukaryotes, actin is the major cytoskeletal component that provides the structural basis for growth polarity (Bretscher *et al.*, 1994). During polarized growth, actin filaments are oriented toward the site at which the new bud will emerge and there is a concentration of actin patches at the bud site (Adams and Pringle, 1984). In conditional *CDC42* mutants, or in other conditional mutants defining genes required for regulating Cdc42p activity, growth at the restrictive temperature results in formation of unbudded multinucleate cells with a uniform distribution of actin patches and delocalized deposition of chitin, a component of the cell wall (Adams *et al.*, 1990).

In contrast to the situation in *S.cerevisiae*, little is known regarding the molecular mechanisms controlling growth polarity of filamentous fungi. Unlike *S.cerevisiae*,

growth polarity in filamentous fungi is not restricted to a specific phase of the cell cycle (i.e. bud emergence), but is continuous throughout the fungal colony. Hyphal growth is a dynamic process that is responsive to extracellular cues such as mating pheromone and light (Bistis, 1981; Bistis, 1983; Degli-Innocenti *et al.*, 1983; Harding and Melles, 1983). In addition, coordinated growth of numerous hyphal tips is required for formation of complex multicellular structures associated with sexual and asexual reproduction (Turian and Bianchi, 1972; Johnson, 1976; Raju, 1980; Read, 1983; Springer and Yanofsky, 1989). Filamentous fungi are also major pathogens of plants and animals, and hyphal growth is modulated by host recognition and by penetration of host tissue (Cole and Hoch, 1991).

Many *N.crassa* mutants have been identified that display altered colony morphology; however, the biochemical basis for the majority of these mutants is still unknown (Garnjobst and Tatum, 1967; Perkins *et al.*, 1982). We initiated studies aimed at understanding the molecular basis of growth polarity by cloning *N.crassa* genes identified as being required for normal hyphal growth (Yarden *et al.*, 1992). Here we report the analysis of *mcb* (microcycle blastoconidiation), the first *N.crassa* conditional mutant examined that is defective in growth polarity when grown at the restrictive temperature. Our results indicate that *mcb* codes for a regulatory subunit of cAMP-dependent protein kinase (PKA), and suggests that the PKA pathway regulates polarized deposition of wall material for hyphal growth. Unexpectedly, we found that polarized deposition of wall material for septation is not disrupted in the *mcb* mutant grown at the restrictive temperature; however, the septa are abnormally located.

Results

mcb, a temperature-sensitive mutation that affects growth polarity in N.crassa

The *N.crassa mcb* mutation was identified in a screen of otherwise wild-type strains that produce precociously either blastoconidia and/or microconidia in liquid medium (Maheshwari, 1991). The *mcb* mutation, which was one of at least two mutant genes in the original strain, was introgressed into an Oak Ridge wild-type background and shown to result in highly distended hyphal growth (Maheshwari, 1991). We examined the introgressed *mcb* mutant in greater detail and found it to be a conditional mutant that is capable of forming defined hyphae at 25°C; however, when shifted to 37°C (restrictive temperature), it shows apolar hyphal growth which is no longer restricted to the apical cell of the hyphal filament (Figure 1). When conidia (asexually derived spores) of *mcb* are inoculated onto a sucrose minimal agar medium and incubated at 25°C, they germinate and give rise to hyphae with swollen tips (Figure 2A). These give rise to a number of bulbous cellular compartments delineated by septa, which in turn generate smaller hyphal tips that develop into typical fungal hyphae (Figures 1A and 2A). When *mcb* hyphae formed at 25°C are shifted to 37°C, or if conidia are germinated at 37°C, growth polarity is lost and all regions of pre-existing hyphae and all germinating conidia grow isotropically until they ultimately burst (Figures 1D and 2B). The tips of *mcb* hyphae shifted to 37°C are the first

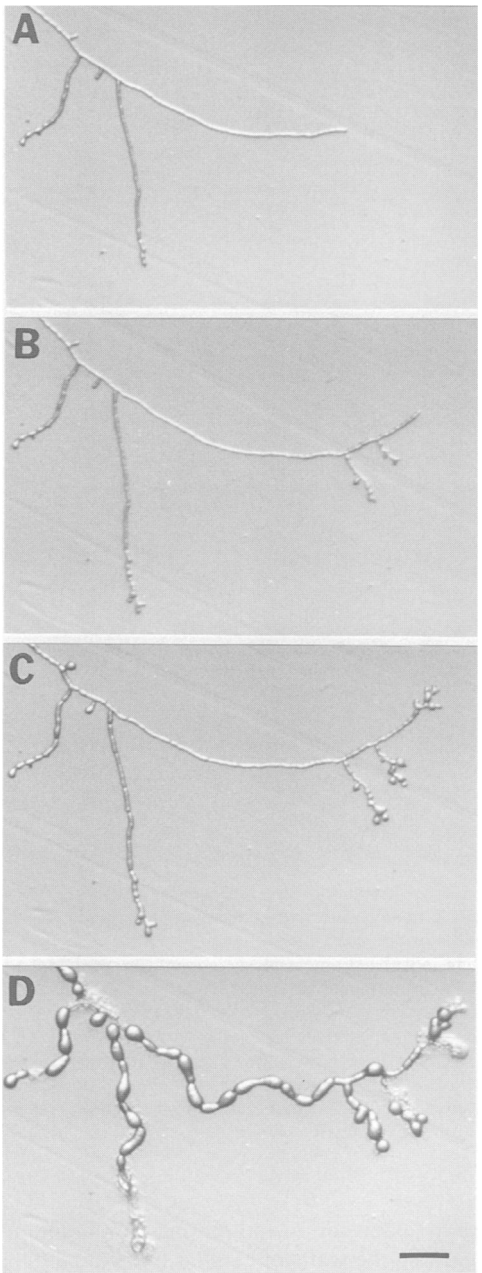

Fig. 1. Loss of growth polarity in the *mcb* mutant shifted to the restrictive temperature (37°C). Conidia from the *mcb* mutant were inoculated onto dialysis membrane overlying sucrose minimal agar medium and incubated overnight (18 h) at 25°C. Hyphae of the *mcb* mutant subsequently were incubated at 37°C by transferring the dialysis membrane to pre-warmed sucrose minimal agar medium. (**A**) Hyphae of the *mcb* mutant after overnight incubation at 25°C. The same hyphae shown in (A) were shifted to 37°C and photographed after 1.5 h (**B**), 3 h (**C**) and 9 h (**D**). Note the loss of growth polarity in all regions of *mcb* hyphae grown for 9 h, and that apolar growth continues until hyphal compartments burst (D). Bar indicates 100 μm.

regions of hyphae exhibiting a loss of growth polarity, followed quickly by initiation of apolar growth by all distal regions of hyphae (Figure 1C–D). Apolar growth of *mcb* hyphae shifted to 37°C results in an increase in hyphal length as well as in hyphal diameter (Figure 1D).

Three observations support our hypothesis that the distended cellular units observed in the *mcb* mutant grown at the restrictive temperature arise from isotropic wall growth as opposed to uniform weakening of cell wall

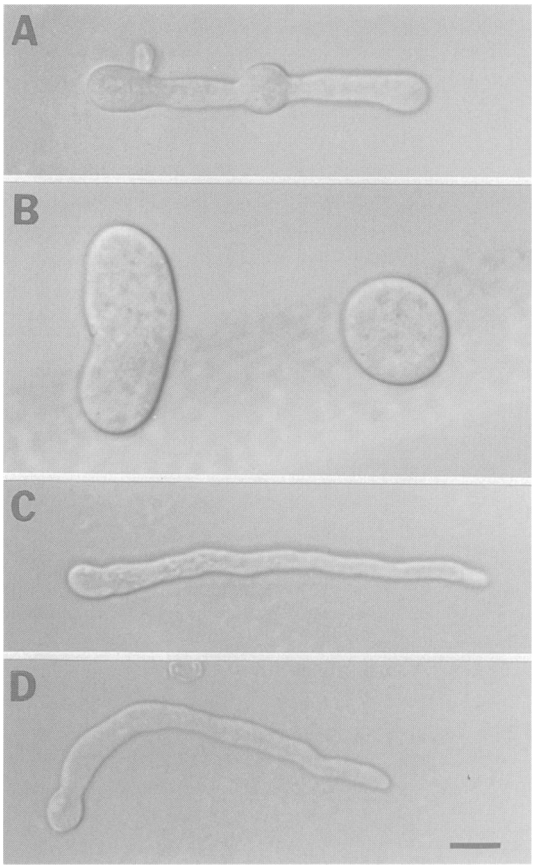

Fig. 2. *cr-1*, a mutant defective in adenylate cyclase, is epistatic to *mcb*. Conidia of the *mcb* and *cr-1* mutants and the *mcb*; *cr-1* double mutant were inoculated onto dialysis membranes overlying sucrose minimal agar medium and incubated for 8 h at either 25 or 37°C. (**A**) An *mcb* germling growing at 25°C. (**B**) Two *mcb* conidia germinated at 37°C. Note the absence of growth polarity. (**C**) A *cr-1* germling growing at 37°C. *cr-1* germlings are indistinguishable from wild-type at this stage of growth. (**D**) An *mcb*; *cr-1* double mutant germling growing at 37°C. Note that the *cr-1* mutation is completely epistatic to the *mcb* mutation (D versus B and C). Bar indicates 5 μm.

followed by extension of the plasma membrane by turgor pressure. First, the walls of cellular units of *mcb* that burst after prolonged growth at 37°C can be seen as thick shells on the dialysis membrane (Figure 1D). The wall can be as thick as 1 μm; this is readily observed during immunolocalization of actin (Figure 6G). Second, as part of our indirect immunofluorescence protocol, a mixture of hydrolytic enzymes (Novozyme 234 LP) is used to digest the cell wall prior to incubation with primary and secondary antibodies (see Materials and methods). Hyphae of the *mcb* mutant transferred to the restrictive temperature must be digested >8-fold longer to allow antibodies to penetrate the wall. Finally, fungal mutants have been isolated that are defective in wall integrity, and the morphological defects and lysis of these mutants can be prevented by osmotic stabilization of the growth medium (Cid *et al.*, 1995). The addition of 1 M sorbitol to the growth medium of an *mcb* mutant incubated at 37°C does not restore a wild-type growth phenotype, nor does it prevent or delay lysis, suggesting that there is not a general loss of cell wall integrity in the *mcb* mutant incubated at 37°C.

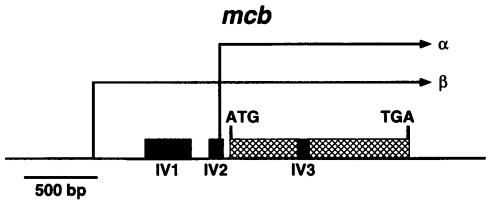

Fig. 3. Structure of the *mcb* gene. The *mcb* gene consists of two overlapping transcription units (α and β, indicated by arrows). The longest transcript (β) is interrupted by three introns [IV1 (288 bp), IV2 (73 bp) and IV3 (67 bp)]. The first two introns (IV1 and IV2) are located within the non-translated 5′ leader sequences of the β transcript. The third intron is located inside the coding region of the gene (filled box). The short transcript (α) is initiated within the IV2 of the β transcript and is interrupted by only one intron (IV3). The predicted *mcb* structural gene consists of a 385 codon open reading frame (hatched box). The nucleotide sequence data reported in this paper will appear in the EMBL, GenBank, and DDBJ Nucleotide Sequence Databases under the accession number L78009.

Cloning, mapping and structural organization of the N.crassa mcb gene

A sib selection protocol was used to identify cosmid clones capable of complementing the recessive *mcb* defect. Complementation was defined as restoration of polar growth (i.e. formation of straight, rapidly extending hyphae) of the *mcb* mutant, grown at the restrictive temperature. One cosmid, X13C10, was identified and its map position was determined by restriction fragment length polymorphism (RFLP) analysis to be between two markers (*cyh-2* and *vma-1*) that are closely linked to the known position of the *mcb* mutation. This suggests that complementation resulted from introduction of a wild-type copy of the *mcb* gene and not from introduction of an unlinked gene capable of suppressing *mcb* by virtue of an increased dosage or an ectopic location.

The location of the *mcb*-complementing activity within cosmid X13C10 was determined by digesting the cosmid with various restriction endonucleases and transforming the *mcb* strain with the resulting fragments. (*N.crassa* is transformed efficiently with linear DNA.) Restriction endonucleases that cut within the insert DNA of cosmid X13C10, but did not eliminate complementing activity, were used to subclone the *mcb* gene. *mcb*-complementing activity was localized to a 3.5 kbp *Xba*I–*Sac*I fragment, and the DNA sequence of 3.3 kbp of this fragment was determined (Sanger *et al.*, 1977). Examination of the DNA sequence of this fragment revealed a 385 codon open reading frame (ORF) interrupted by a 67 bp intron (IV3; Figure 3). Restriction endonucleases that cut within the 385 codon ORF inactivated complementing activity, including endonucleases that cut exclusively within this region.

Northern analysis showed two distinct *mcb* mRNAs (Figure 4), indicating two apparent transcription start sites for the *mcb* gene (Figure 3). This was consistent with the analysis of *mcb* cDNAs. The 5′ end of the longer *mcb* mRNA (β) was located ~950 bp upstream of the putative translation initiation codon of the *mcb* structural gene. Two introns were identified within this long leader region (IV1 and IV2; Figure 3). The 5′ end of the shorter *mcb* mRNA (α) was within sequences comprising the second intron (IV2; Figure 3). Stop codons were located in all reading frames of the leader regions of the β and α transcripts, indicating that both mRNAs probably encode

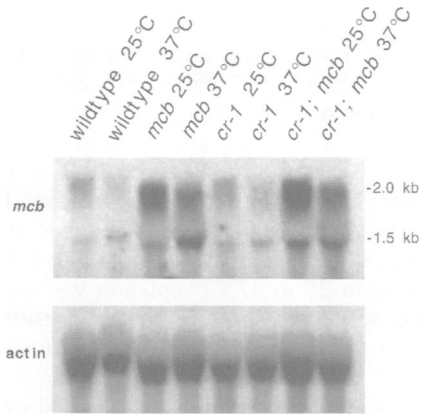

Fig. 4. Analysis of *mcb* transcript levels. *mcb* transcript levels were examined in *mcb*$^+$ (wild-type), in *mcb* and *cr-1* mutants and in the *mcb*; *cr-1* double mutant grown in sucrose minimal liquid medium at 25°C for 8 h or at 25°C for 6 h and then shifted to 37°C for an additional 2 h. Total RNA was isolated from each culture and a Northern blot of gel-fractionated RNA (30 μg per lane) was hybridized with an *mcb*$^+$-specific probe (1.3 kbp *Bam*HI fragment). Equal loading and transfer of RNA was examined by stripping the *mcb*$^+$-probed blot and reprobing it with a cDNA clone corresponding to the *N.crassa* actin gene.

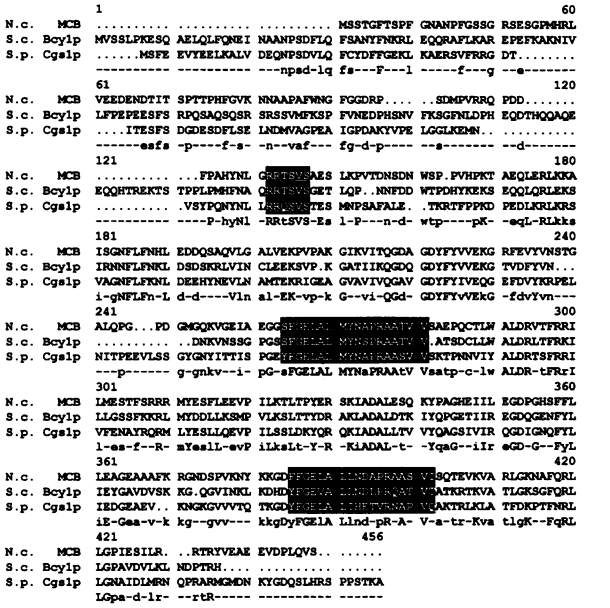

Fig. 5. Comparison of the predicted amino acid sequence of *N.crassa* MCB with the PKA regulatory subunits of *S.cerevisiae* (Bcy1p; Toda *et al.*, 1987) and *S.pombe* (Cgs1p; DeVoti *et al.*, 1991). The alignment was made using the UWGCG program PILEUP. Gaps (indicated by dots) were introduced to maximize the alignment. Lower and upper case letters under the sequence alignment indicate residues that are either identical in two of the three (lower case) or in all three proteins (upper case). Three conserved domains within the aligned PKA regulatory subunits are boxed. The first domain is a six residue sequence (RRtSVS) that acts as the kinase inhibitor domain, and the two distal highlighted sequences represent cAMP binding domains (Taylor *et al.*, 1990).

identical protein products. In addition, the only ATG sequences located immediately upstream of the putative translation initiation codon of the *mcb* structural gene were within the first intron (Figure 3) and, therefore, were not present even in the longer of the two *mcb* mRNAs.

To investigate transcriptional regulation of the *mcb* gene, we examined *mcb* transcript levels in wild-type (*mcb*$^+$) and *mcb* strains and found that *mcb* transcripts are more abundant in the *mcb* mutant than in the wild-type strain (Figure 4). In addition, wild-type and *mcb* strains, shifted from a growth temperature of 25 to 37°C, showed a decrease in the level of the longer transcript (β) and a slight increase in the amount of the shorter transcript (α) (Figure 4). This indicates that the *mcb* phenotype is not due to a reduction in the levels of *mcb* transcript and also suggests that the levels of the two *mcb* transcripts are not coordinately regulated.

mcb encodes a regulatory subunit of cAMP-dependent protein kinase

mcb is predicted to encode a 385 amino acid polypeptide with a calculated mass of 42 kDa. A comparison of the predicted amino acid sequence of MCB with sequences in the database revealed that MCB has similarity to PKA regulatory subunits (Altschul *et al.*, 1990). MCB is 45 and 39% identical, and 62 and 57% similar, to the PKA regulatory subunits of *S.cerevisiae* (Bcy1p) and *S.pombe* (Cgs1p), respectively, and ~35% identical to various vertebrate regulatory subunits (Figure 5). Low stringency Southern and Northern analyses identified only *mcb* sequences, suggesting that *N.crassa* has only one gene encoding a PKA regulatory subunit.

Extensive work has been done on PKA in a variety of experimental systems (for review, see Taylor *et al.*, 1990). PKA consists of two regulatory subunits that bind to and inhibit the activity of two catalytic subunits. In the presence of cAMP, the regulatory subunits dissociate from the catalytic subunits, resulting in free catalytic subunits which are the active kinase. Three major structural features are present within the regulatory subunit. A dimerization domain is located in the N-terminal one-third of the protein and has been shown to mediate dimer formation between two regulatory subunits and interaction with other cellular proteins. This region is not highly conserved between various regulatory subunits, including MCB (Figure 5). The kinase inhibitor domain is a highly conserved six residue sequence (RRtSVS) that acts as an inhibitor of catalytic subunit kinase activity and also mediates interaction between the regulatory and catalytic subunits. This domain is conserved in MCB (Figure 5). Two near-duplicate cAMP binding domains are also found in typical regulatory subunits, and both cAMP binding domains are present in MCB (Figure 5). From the sequence similarity and conservation of domains found in previously studied regulatory subunits, we conclude that MCB is a *Neurospora* regulatory subunit of PKA.

An adenylate cyclase mutation, crisp-1 (cr-1), is epistatic to the mcb mutation

A preliminary indication of the nature of the *mcb* mutation came from selection of suppressors that allowed polar growth at the restrictive temperature. Conidia of *mcb inl* were irradiated with UV light (258 nm) to ~40% killing, plated to agar medium with inositol, and incubated at 40°C for 3 days. Among 65 suppressed or reverted strains picked, two showed a very distinctive morphology characteristic of the long recognized mutant *cr-1* (Perkins *et al.*, 1982). Outcrosses of these showed that the original *mcb* mutation segregated among the progeny, and thus polarized growth of the *mcb*-derived parent at 40°C was

due to a suppressor mutation, not to reversion of *mcb*. A cross of one of the two suppressed strains to *cr-1* (allele B123 from the FGSC) gave only *crisp* progeny among >700 colonies from germinated ascospores. The lack of progeny with an *mcb* phenotype suggests that the suppression of *mcb* was due to a newly arisen mutation at the *cr-1* locus. A forced heterokaryon between the suppressed *mcb inl* strain and *cr-1*; *pan-2* was made by mixing conidia of the two strains on minimal medium at the permissive temperature. The morphology of the heterokaryon was typical of *cr-1*, and was indistinguishable from that of either component growing on nutritionally permissive medium. Thus the suppressed *mcb* strain carries a suppressor mutation of the *cr-1* locus that is also functionally identical with *cr-1*; the new *cr-1* mutation was designated as allele 28.

The *cr-1* locus encodes adenylate cyclase (Terenzi *et al.*, 1976; Kore-eda *et al.*, 1991). In *cr-1* mutants, cAMP levels are reduced or are below detection (Terenzi *et al.*, 1976). A comparison of the growth of *mcb* and *cr-1* mutants, and the *mcb*; *cr-1* double mutant is shown in Figure 2. *mcb* germlings grown from conidia at 25°C exhibit polar growth, though hyphal tips are swollen during the initial stages (Figure 2A). At 37°C, *mcb* conidia grow into spheres that enlarge in an apolar fashion and ultimately burst (Figure 2B). *cr-1* and *mcb*; *cr-1* germlings, by contrast, form hyphae that are indistinguishable from those of wild-type (Figure 2C and D).

Northern analysis was used to examine the effect of the *cr-1* mutation on *mcb* transcript levels (Figure 4). In the *cr-1* mutant, both *mcb* transcripts (α and β) were observed at approximately the same levels as seen in the wild-type strain. In the *mcb*; *cr-1* double mutant, *mcb* transcript levels were similar to those observed in the *mcb* mutant (Figure 4). Therefore, even though *cr-1* is epistatic to *mcb*, it does not lead to a reduction in *mcb* transcript levels to those seen in wild-type.

Analysis of cytoskeleton organization and septation in mcb$^+$ and mcb strains

Actin is the major cytoskeletal component functioning in polarization of cell growth (Bretscher *et al.*, 1994; Drubin and Nelson, 1996). In filamentous fungi, new cell wall growth occurs primarily at hyphal tips, and visualization of actin in hyphae of a wild-type strain showed that there is a concentration of actin patches at hyphal tips (Figure 6A). Adjustment of the focal plane of the microscope so that it bisected hyphae revealed that actin patches localized to hyphal tips were associated with the cell cortex (Figure 6B). The distribution of actin patches in the *mcb* mutant growing at the permissive temperature (25°C) was similar to that of the wild-type strain, although there was a 3-fold increase in the diameter of *mcb* mutant hyphae (Figure 6D and E). When *mcb* hyphae were shifted to the restrictive temperature (37°C), growth became apolar and actin patches were uniformly distributed over the surface of hyphae (Figure 6G). Introduction of a *cr-1* mutation into the *mcb* strain restored polar growth at 37°C, and actin patches were again concentrated at hyphal tips (Figure 6I and J).

Cellularization of fungal hyphae occurs by septation, an actin-dependent process (Patton and Marchant, 1978; Girbardt, 1979; Harris *et al.*, 1994). In wild-type *N.crassa* and in the *mcb* mutant grown at 25°C, actin localized to sites of septum formation is organized as a collection of patches or as a dense band (Figure 6C and F). Over half of the septa being formed in the *mcb* mutant were observed to have a double ring of actin patches (Figure 6F); however, these structures were seen <10% of the time in the wild-type. [Double rings of actin patches have also been observed at sites of septation in other filamentous fungi (Salo *et al.*, 1989; Harris *et al.*, 1994).] When *mcb* was shifted from 25 to 37°C, septation was not blocked (Figure 6G; see below). Large spheres, resulting from apolar growth, were often spanned by a septum, indicating that initiation of septation and deposition of materials required for septum formation had continued even in the absence of polar growth (Figure 6G and H). Actin rings associated with septation were observed in *mcb* growing at 37°C; however, the relative positions of actin rings with respect to each other and to the hyphae were altered (Figure 6H).

We examined septation more closely by staining with calcofluor, which identifies chitin and other β-linked polysaccharides found in mature septa (Darken, 1961; Maeda and Ishida, 1967). In *mcb* grown at 25°C, and in *cr-1* and *mcb*; *cr-1* grown at 37°C, calcofluor staining revealed that septa were distributed throughout hyphae in approximately the same manner as in a wild-type strain (Figure 7A versus B, C and D). In mature hyphae, septa were located at intervals of 55 ± 25 μm and, typically, septal formation began 100–180 μm behind the hyphal apex (Hunsley and Gooday, 1974). The septa shown in Figure 7A–D were exceptional in that they were located only 30–40 μm behind their respective hyphal tips. These hyphae were chosen to illustrate chitin distribution over the entire distance from a hyphal tip to a septum. *mcb* shifted to 37°C was able to form septa; however, the placement of the septa was abnormal (Figure 7E–H). Two to three septa could be observed immediately adjacent to each other (Figure 7E, G and H), and septa occasionally were formed at oblique angles with respect to the long axis of a hypha (Figure 7G). Many of the spherical cells that result from apolar growth of the *mcb* mutant incubated at 37°C were completely spanned by a septum (Figure 7F). Septa located within spherical cells bisected spheres only occasionally; most septa traversing spherical cells did so in an asymmetrical fashion.

Cytoplasmic microtubules have been proposed to be required for long-range transport of vesicular cargo required for the formation of cell wall and hyphal tip extension (Howard, 1981). In wild-type, cytoplasmic microtubule tracks were seen to be located in all regions of hyphae (Figure 8B). Some of the microtubule tracks were >50 μm in length and extended from distal regions of hyphae to the hyphal apices. The organization of cytoplasmic microtubules in the *mcb*, *cr-1*, and in the *mcb*; *cr-1* double mutant did not differ from that of wild-type, although hyphae of the *mcb* mutant grown at 25°C were considerably thicker than those of the other strains (Figure 7D, H and J). The organization of cytoplasmic microtubules in *mcb* shifted to 37°C differed significantly from that of other strains examined (Figure 8F). In *mcb* shifted to the restrictive temperature, cytoplasmic microtubule tracks were generally shorter than those observed in distinct hyphae, and they were organized as

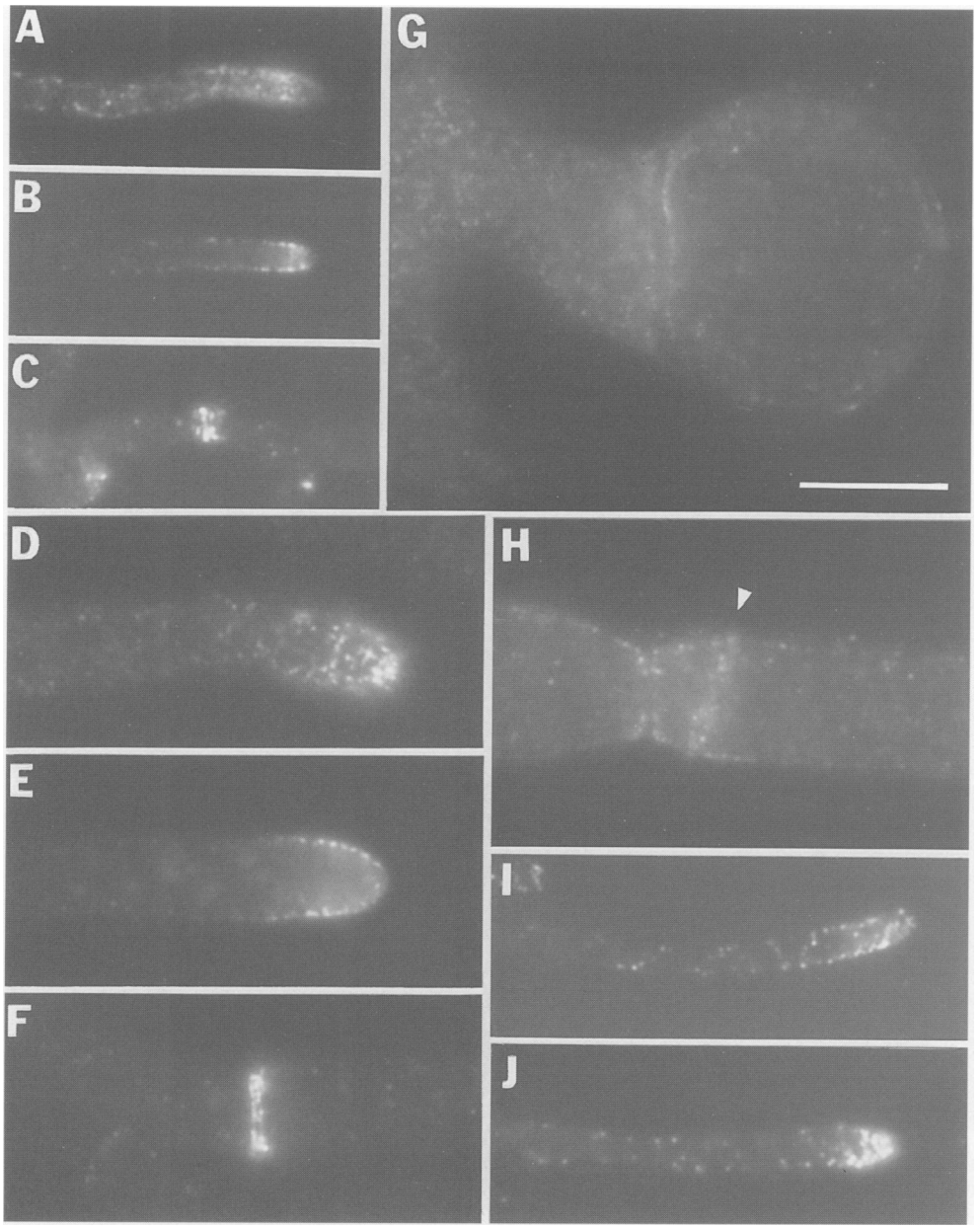

Fig. 6. Actin organization in mcb^+ (wild-type), in *mcb* and *cr-1* mutants and in the *mcb*; *cr-1* double mutant. Conidia were inoculated onto filters placed on sucrose minimal agar medium and the plates were either incubated for 24 h at 25°C or for 18 h at 25°C followed by an additional 6 h at 37°C. The samples were processed for indirect immunofluorescence using an anti-actin antibody as described in Materials and methods. (**A**), (**B**) and (**C**) mcb^+ (wild-type) at 25°C; (**D**), (**E**) and (**F**) *mcb* at 25°C; (**G**) and (**H**) *mcb* shifted to 37°C; (**I**) *cr-1* shifted to 37°C; and (**J**) *mcb*; *cr-1* shifted to 37°C. A concentration of actin patches at tips of hyphae is visible in (A), (D), (I) and (J). Association of actin patches with the cortex, observed by adjusting the focal plane of the microscope so that it bisects hyphae, is seen in (B) and (E). Actin organization associated with septation is shown in (C), (F), (G) and (H). Note the presence of two rings of actin at or near the point of septation (F), the uniform distribution of cortical actin patches and the large septum spanning a distended hypha (G) and the presence of an actin ring that spans a hypha at an oblique angle and is localized near a septum that was formed earlier in the *mcb* strain (arrow, H). Bar indicates 10 μm.

extensive, overlapping networks. Careful adjustment of the focal plane of the microscope revealed that most of the cytoplasmic microtubules were associated with the cell cortex. Occasionally, a spherical cell had a high concentration of microtubules at one site of the cell cortex (Figure 8F). Nuclei were relatively evenly distributed in all strains examined; however, as with microtubules, nuclei were associated primarily with the cell cortex in the large spherical cells of the *mcb* mutant incubated at 37°C (Figure 8). There are many more nuclei per unit length of hypha in the *mcb* mutant growing at the permissive temperature compared with the wild-type control (Figure 8C versus A); however, these nuclei are distributed evenly and also excluded from hyphal tips, which is typical of most fungi (McKerracher and Heath, 1987).

Discussion

More than 100 *N.crassa* mutants with altered colonial morphology have been isolated by simple visual screens (Garnjobst and Tatum, 1967; Perkins *et al.*, 1982). *mcb* is the first *N.crassa* mutant to be analyzed that is defective in growth polarity. Transfer of *mcb* hyphae from 25 to 37°C resulted in loss of growth polarity at hyphal tips

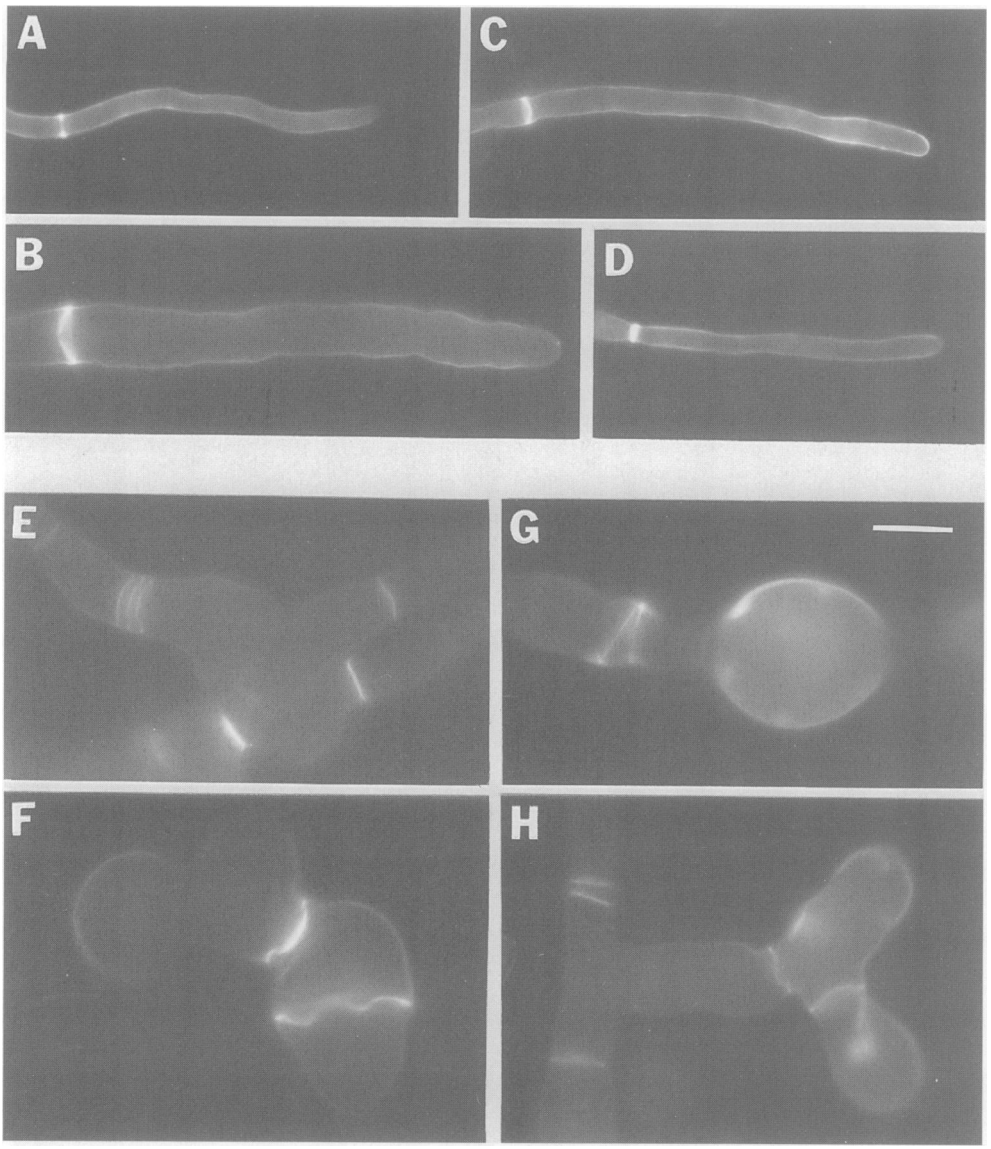

Fig. 7. Chitin localization in mcb^+ (wild-type), in *mcb* and *cr-1* mutants and in the *mcb*; *cr-1* double mutant. Strains were grown as described for immunolocalization of actin (Figure 6) and stained with calcofluor to reveal chitin organization. (**A**) mcb^+ (wild-type) at 25°C; (**B**) *mcb* at 25°C; (**C**) *cr-1* at 37°C; (**D**) *mcb*; *cr-1* at 37°C; and (**E**), (**F**), (**G**) and (**H**) *mcb* shifted to 37°C. Hyphae presented in (A–D) were chosen to show calcofluor staining of septa and hyphal tips. (E–H) Calcofluor staining of chitinous structures in *mcb* hyphae and tip cells after a 6 h shift to 37°C. Note the patches of chitinous material on the surfaces of spherical cells (G and H) the close positioning of multiple septa (E, G and H), the oblique positioning of septa with respect to the long axis of a hypha (G) and the presence of septa spanning large spherical cells formed by apolar growth (F). Bar indicates 10 μm.

and initiation of isotropic growth in distal segments of hyphae (Figure 1). In contrast, polarized deposition of wall material in regions of septation was not blocked in the *mcb* mutant incubated at 37°C (Figures 6 and 7). These findings indicate that, while both polarized growth and septation require organized actin and synthesis of new cell wall, these two processes are subject to independent regulatory mechanisms. Numerous mutants that have lost the ability to form septa have been identified in filamentous fungi; however these mutants still grow in a polarized fashion (Morris, 1976; Harris *et al.*, 1994). *mcb* is unique in that it represents a mutant defective in polarized hyphal growth, but one still capable of forming septa. Septation occurred in all regions of hyphae of the *mcb* mutant that were growing isotropically; however, the placement of these septa was clearly abnormal (Figures 6 and 7). Our finding that the *mcb* gene encodes a regulatory subunit of PKA implicates the PKA pathway as a regulator of polarized hyphal growth and perhaps localization of septa.

Unlike *N.crassa*, *S.cerevisiae* PKA regulatory mutants (*bcy1*) are relatively unaffected in growth morphology. Hyperactivation of *S.cerevisiae* PKA by a *bcy1* mutation results in an increase in cell size prior to commitment to a new round of cell division, stimulation of pseudohyphal growth and a variety of physiological changes (Gimeno *et al.*, 1992; Mitsuzawa, 1994); however, it does not lead to a loss of growth polarity as seen in the *N.crassa mcb* mutant. The reason for this discrepancy is unknown, but it may result from the very different ways in which these two fungi grow and form septa. In *S.cerevisiae*, polarized growth is restricted to a short phase of the cell cycle and is intimately associated with the formation of the septum (for review, see Cid *et al.*, 1995). In filamentous fungi like *N.crassa*, septation and polarized growth are not

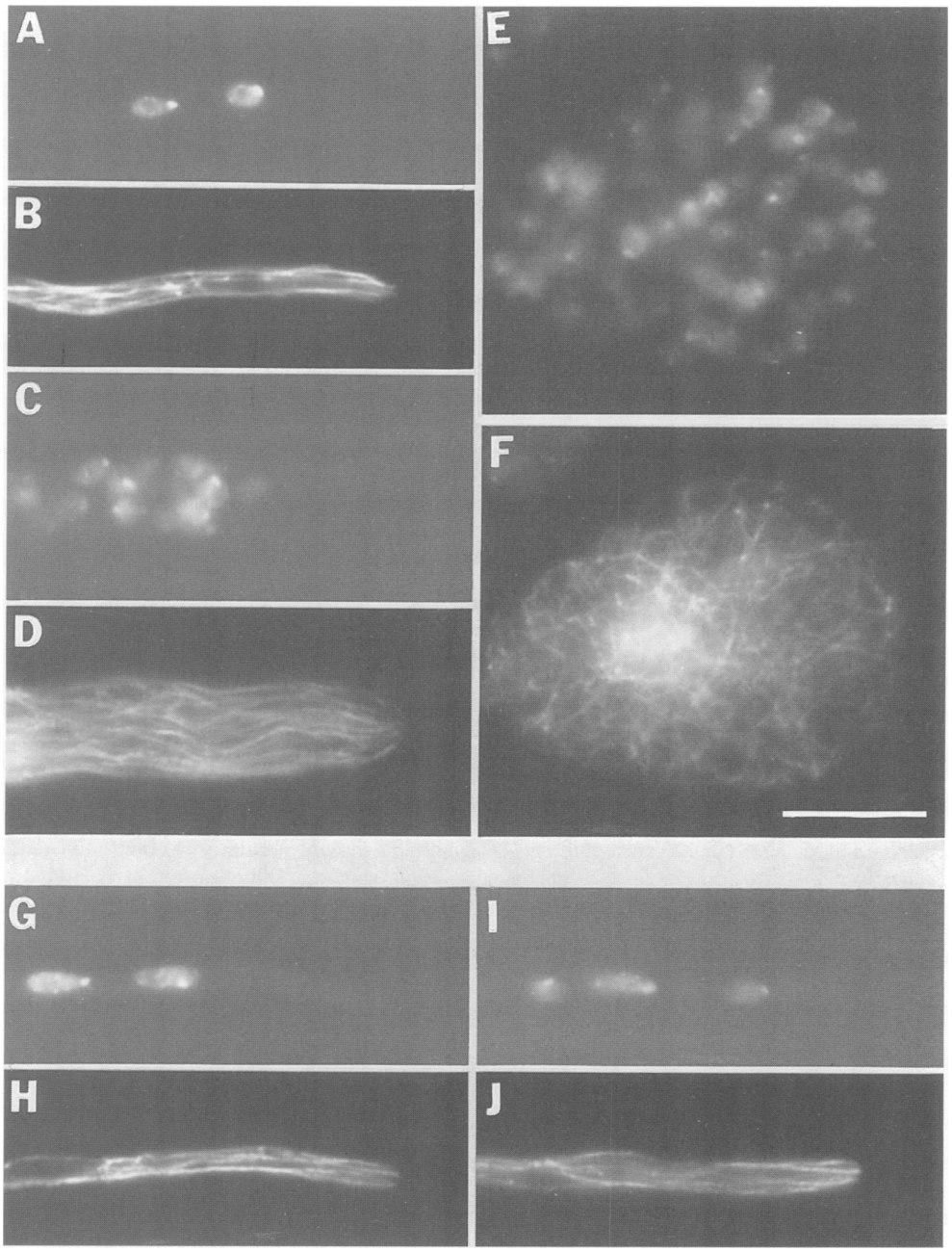

Fig. 8. Microtubule organization and distribution of nuclei in mcb^+ (wild-type), in *mcb* and *cr-1* mutants and in the *mcb*; *cr-1* double mutant. Strains were grown as described in Figure 6, processed for indirect immunofluorescence using an anti-α-tubulin antibody to visualize microtubules, and stained with DAPI to visualize nuclei (see Materials and methods). (**A**) and (**B**) mcb^+ (wild-type) at 25°C; (**C**) and (**D**) *mcb* at 25°C; (**E**) and (**F**) *cr-1* shifted to 37°C; and (**G**) and (**H**) *mcb*; *cr-1* shifted to 37°C. Nuclear distribution is presented in (A), (C), (G) and (I). The corresponding view of microtubules in shown in (B), (D), (H) and (J). Bar indicates 10 μm.

coupled processes, and septation does not formally divide hyphae into independent growth units as it does in *S.cerevisiae* (Hunsley and Gooday, 1974; Harris *et al.*, 1994). It is possible that the gross morphological changes observed in the *N.crassa* PKA regulatory subunit mutant, but not in the corresponding *S.cerevisiae* mutant, result from these differences. We propose that increased PKA activity results in failure to organize actin at the hyphal apex, but not at sites of septation, with the result that actin patches are uniformly distributed around the cortex. Therefore, filamentous fungi lacking PKA regulatory subunit function grow until they lyse because either they fail to increase the surface area of the cellular unit to keep pace with their increase in volume or because they cannot utilize the process of septation to adequately control the size of the cellular unit. In contrast, budding fungi like *S.cerevisiae* survive hyperactivation of PKA because coupling of septation and bud emergence (PKA-independent events) prevents cells from exceeding a critical volume.

Recent work on dimorphic switching in the corn pathogen *Ustilago maydis* and appressorium formation in the rice pathogen *Magnaporthe grisea* also suggests that cAMP and the PKA pathway play a general role in controlling polarized versus isotropic cell wall growth in filamentous fungi (Gold *et al.*, 1994; Mitchell and Dean,

1995). In *U.maydis*, activated PKA results in a constitutive budding (yeast-like) mode of growth, while loss of cAMP production by disruption of the adenylate cyclase gene results in constitutive filamentous growth (Gold *et al.*, 1994). In *M.grisea*, a spore germinates on the surface of a rice leaf and forms a germ tube which then undergoes delocalized growth to form a spherical structure, the appressorium, that is required for penetration of plant tissue (Cole and Hoch, 1991). Disruption of the gene encoding the catalytic subunit of the PKA of *M.grisea* does not interfere with normal polarized growth; however, appressorium formation is eliminated or severely reduced (Mitchell and Dean, 1995). These results are consistent with our proposal that increased PKA activity results in delocalized cell wall growth, and is perhaps required for it.

Ustilago maydis and *M. grisea* are fungi which activate the PKA pathway as a means of enacting a developmental switch which affects growth polarity in a very controlled and consistent manner. *Neurospora crassa* is neither a dimorphic fungus nor a plant pathogen; however, there is evidence that the PKA pathway does control asexual reproduction (conidiation) in *Neurospora*. Because conidiation can be viewed as an alteration of growth polarity resulting in the formation of chains of conidia (Springer and Yanofsky, 1989), one possible interpretation of the *mcb* phenotype is that a defect in the regulatory subunit of PKA results in induction of the conidiation pathway leading to a loss of growth polarity. There are two reasons why we believe this is not the case. First, the *Neurospora cr-1* gene encodes adenylate cyclase and *cr-1* mutants produce an abundance of conidia once exposed to air. In contrast, the *mcb* mutation, growing at permissive temperatures, shows delayed conidiation, and it is only when the *cr-1* mutation is introduced into the *mcb* strain that one observes hyperconidiation. Second, genes have been identified that are expressed exclusively during conidiation (Berlin and Yanofsky, 1985; Lauter *et al.*, 1992), and we have determined that the expression of two of these genes, *eas* and *con-10*, is not induced when the *mcb* mutant is transferred to the restrictive temperature (data not shown).

One of the most remarkable phenotypic changes that occurs in the *mcb* mutant is the mislocalization of septa (Figures 6 and 7). In *N.crassa*, septa are typically formed perpendicular to the long axis of the hypha and are spaced at intervals of 55 ± 25 μm during vegetative growth (Hunsley and Gooday, 1974). However, in the *mcb* mutant shifted to 37°C, septa are observed at oblique angles to what was formerly the long axis of the hypha, and two to three septa are occasionally formed next to each other as if there were multiple rounds of septation at one site. In *S.cerevisiae* and *S.pombe*, cortical cues are thought to mark the site at which septation will occur (Chang and Nurse, 1996; Chant, 1996). It is possible that isotropic cell wall growth observed in the *mcb* mutant disrupts a cortical marker such that septation becomes random with respect to the axis of hyphal growth and position of adjacent septa. Alternatively, the PKA pathway may play a direct role in establishing sites for septation in *N.crassa*. Actin patches are uniformly distributed over the cell cortex when the *mcb* mutant is incubated at the restrictive temperature, suggesting that the PKA pathway regulates cortical actin organization. If the marker establishing sites for septation is dependent on properly organized cortical actin, then placement of septa, as well as polarity of growth, would be lost in the *mcb* mutant grown at 37°C.

Given the importance of growth polarity, one might expect intricate regulation of *mcb* gene expression. The presence of two distinct *mcb* transcripts suggests that *mcb* has two promoters and is subject to complex transcriptional control (Figures 3 and 4). The levels of both *mcb* transcripts are elevated in the *mcb* mutant relative to wild-type. This increase indicates that there is a feedback mechanism controlling the level of PKA regulatory subunit, probably in response to the levels of active PKA catalytic subunit. It is likely that the increased *mcb* transcript levels observed in the *mcb* mutant result from an effort to control the activity of the PKA catalytic subunit by increasing production of the partially active regulatory subunit. Similar regulatory responses have been observed in *S.cerevisiae* and *S.pombe* (Zoller *et al.*, 1988; DeVoti *et al.*, 1991). When *mcb* or wild-type is transferred from an incubation temperature of 25°C to 37°C, there is an increase in the level of the shorter message (α) and a decrease in the longer message (β). This result suggests that the two promoters are regulated, at least in part, independently. Introduction of a *cr-1* mutation into the *mcb* mutant restores growth polarity, but does not reduce the levels of *mcb* transcripts. One interpretation of these results is that the *mcb* mutation severely reduces the effectiveness of the PKA regulatory subunit to inhibit PKA catalytic subunit activity, and it is only through increasing production of mutant regulatory protein and reduction in cAMP levels that the mutant protein is able to regulate PKA activity adequately and allow polarized growth.

The striking morphological effects of mutations in the *N.crassa* PKA regulatory subunit relative to the corresponding mutations in *S.cerevisiae* and *S.pombe* (Toda *et al.*, 1987; DeVoti *et al.*, 1991) makes *N.crassa* a productive system for exploring the mechanisms by which the PKA pathway regulates growth polarity and placement of septa. Suppressor mutations that restore growth polarity to the *mcb* mutant when it is incubated at 37°C, but do not directly affect the PKA pathway (e.g. *cr-1* mutations), may lead to the identification of genes that are responsive to PKA activity and regulate actin organization at the cell cortex.

Materials and methods

Strains and media

The following *N.crassa* strains were obtained from the FGSC (Fungal Genetics Stock Center, Department of Microbiology, University of Kansas Medical Center, Kansas City, KS): FGSC 987 [wild-type (*mcb*$^+$) 74-OR23-1A], FGSC 7094 (*mcb*) and FGSC 4008 [*cr-1* (B123)]. The *cr-1* (28); *mcb*, *inl* (89601) strain was constructed during this study. Media, growth conditions, sexual crosses and formation of heterokaryons were done using standard procedures (Davis and de Serres, 1970). DNA-mediated transformations were performed as described (Vollmer and Yanofsky, 1986).

Cloning and sequencing of mcb genomic and cDNA clones

Sib selection was used to identify cosmid clones from the Orbach/Sachs cosmid library (FGSC) capable of complementing the growth defect of *mcb* incubated at 37°C (Vollmer and Yanofsky, 1986). The map location of the identified cosmid (X13C10) was determined by RFLP analysis (Metzenberg *et al.*, 1985).

DNA sequencing was performed by the dideoxy chain termination method (Sanger *et al.*, 1977), using Sequenase version 2.0 (United

States Biochemical, Cleveland, OH) and custom oligonucleotide primers synthesized by the Gene Technologies Laboratory at Texas A&M University. DNA sequences were analyzed using programs of The University of Wisconsin Genetics Computer Group (Devereux *et al.*, 1984). GenBank searches were performed at the National Center for Biotechnology Information (Bethesda, MD), using the BLAST network service (Altschul *et al.*, 1990).

cDNA clones of *mcb*$^+$ were isolated by screening ~1×10^6 plaques from two λ ZAP® II *N.crassa* (nitrate-induced and glutamine-repressed) cDNA libraries constructed by R.H.Garrett (University of Virginia, Charlottesville, VA) and available through the FGSC. For a probe, we used a 0.9 kbp gel-isolated fragment (*Bam*HI–*Eco*RI fragment). Twenty five phage clones carrying positive cDNAs were identified and purified using described procedures (Sambrook *et al.*, 1989). Phagemids were rescued using ExAssist® helper phage following procedures recommended by the manufacturer (Stratagene, La Jolla, CA). Six cDNAs isolated from the nitrate-induced library were selected for further analysis and their sequences determined as described above.

Standard procedures for Southern and Northern analyses, restriction endonuclease digestions, agarose gel electrophoresis, purification of DNA from agarose gels, DNA ligations and other cloning-related techniques were performed as described (Sambrook *et al.*, 1989). Genomic DNA was isolated from *N.crassa* as described (Yarden *et al.*, 1992). Total RNA was isolated from powdered, freeze-dried mycelia using TRIzol®Reagent according to the manufacturer's instructions (GibcoBRL, Grand Island, NY).

Microscopy

Hyphal morphologies were examined by inoculating the surface of a dialysis membrane overlying sucrose minimal agar medium with conidia of the appropriate strain and incubating plates at designated temperatures and times. Pictures were taken with Kodak Technical Pan film (ASA100) (Rochester, NY) through either an Olympus binocular dissection microscope at 110× magnification with transmitted light or with an Olympus microscope using a SPlan Apo 40× objective and differential interference contrast optics.

Actin and microtubule organization was determined using indirect immunofluorescence as described (Tinsley *et al.*, 1996). In brief, hyphae of the appropriate strain were grown on small pieces (0.5 cm×0.5 cm) of cellulose filter (GN-6 membrane filter, Gelman Sciences, Ann Arbor, MI), quick-frozen in liquid propane and subjected to low temperature fixation. The hyphae were permeablized by treatment with Novozyme 234 LP (Novo Nordisk Biotech, Inc., Davis, CA) and incubated with respective primary antibodies followed by incubation with appropriate secondary antibodies. Primary antibodies used in this study were: DM1-A monoclonal anti-α-tubulin mouse IgG antibody (used at a 1:100 dilution); and C4 monoclonal anti-actin mouse IgG antibody (used at a 1:400 dilution; both from ICN Biochemicals, Inc., Costa Mesa, CA). Secondary antibody was sheep anti-mouse IgG conjugated to Cy3 (used at a 1:1000 dilution; Sigma, St Louis, MO). Cy3 was observed using a rhodamine filter set.

Examination of nuclei and organization of chitin was conducted by staining quick-frozen, low temperature-fixed hyphae with 1 μg/ml 4′,6-diamidino-2-phenylindole (DAPI) or 1 μg/ml calcofluor (Fluorescent Brightener 28; both from Sigma, St Louis, MO), respectively, as described (Tinsley *et al.*, 1996). Indirect immunofluorescence, DAPI- and calcofluor-stained samples were observed on an Olympus BH-2 microscope with the appropriate epi-illumination filter cube using a 1.3 N.A. 100× oil immersion. Pictures were taken with Kodak Technical Pan film (ASA100).

Acknowledgements

This work was supported by U.S. Public Health Service grants GM51217 to M.P. and GMO8995 to R.L.M.

References

Adams,A.E.M. and Pringle,J.R. (1984) Relationship of actin and tubulin distribution to bud growth in wild-type and morphogenetic-mutant *Saccharomyces cerevisiae*. *J. Cell Biol.*, **98**, 934–945.

Adams,A.E.M., Johnson,D.I., Longnecker,R.M., Sloat,B.F. and Pringle,J.R. (1990) *CDC42* and *CDC43*, two additional genes involved in budding and the establishment of cell polarity in the yeast *Saccharomyces cerevisiae*. *J. Cell Biol.*, **111**, 131–142.

Altschul,S.F., Gish,W., Miller,W., Myers,E.W. and Lipman,D.J. (1990) Basic local alignment search tool. *J. Mol. Biol.*, **215**, 403–410.

Barja,F., Thi,B.N. and Turian,G. (1990) Localization of actin and characterization of its isoforms in the hyphae of *Neurospora crassa*. *FEMS Microbiol. Lett.*, **61**, 19–24.

Berlin,V. and Yanofsky,C. (1985) Isolation and characterization of genes differentially expressed during conidiation of *Neurospora crassa*. *Mol. Cell. Biol.*, **5**, 849–855.

Bistis,G.N. (1981) Chemotropic interactions between trichogynes and conidia of opposite mating-type in *Neurospora crassa*. *Mycologia*, **73**, 959–975.

Bistis,G.N. (1983) Evidence for diffusible, mating-type-specific trichogyne attractants in *Neurospora crassa*. *Exp. Mycol.*, **7**, 292–295.

Bretscher,A., Drees,B., Harsay,E., Schott,D. and Wang,T. (1994) What are the basic functions of microfilaments? Insights from studies in yeast. *J. Cell Biol.*, **126**, 821–825.

Chang,F. and Nurse,P. (1996) How fission yeast fission in the middle. *Cell*, **84**, 191–194.

Chant,J. (1994) Cell polarity in yeast. *Trends Genet.*, **10**, 328–333.

Chant,J. (1996) Septin scaffolds and cleavage plans in *Saccharomyces*. *Cell*, **84**, 187–190.

Cid,V.J., Durán,A., Rey,F.D., Snyder,M.P., Nombela,C. and Sanchez,M. (1995) Molecular basis of cell integrity and morphogenesis in *Saccharomyces cerevisiae*. *Microbiol. Rev.*, **59**, 345–386.

Cole,G.T. and Hoch,H.C. (1991) The fungal spore and disease initiation in plants and animals. Plenum Press, New York, NY.

Darken,M.A. (1961) Applications of fluorescent brighteners in biological techniques. *Science*, **133**, 1704–1705.

Davis,R.H. and de Serres,F.J.D. (1970) Genetic and microbiological research techniques for *Neurospora crassa*. *Methods Enzymol.*, **27A**, 79–143.

Degli-Innocenti,F., Pohl,U. and Russo,V.E.A. (1983) Photoinduction of protoperithecia in *Neurospora crassa* by blue light. *Photochem. Photobiol.*, **37**, 49–51.

Devereux,J., Haeberli,P. and Smithies,O. (1984) A comprehensive set of sequence analysis programs for the VAX. *Nucleic Acids Res.*, **12**, 387–395.

DeVoti,J., Seydoux,G., Beach,D. and McLeod,M. (1991) Interaction between *ran1*+ protein kinase and cAMP dependent protein kinase as negative regulators of fission yeast meiosis. *EMBO J.*, **12**, 3759–3768.

Drubin,D.G. and Nelson,W.J. (1996) Origins of cell polarity. *Cell*, **84**, 335–344.

Gabriel,M. (1984) Karyokinesis and septum formation during the regeneration of incomplete cell walls in protoplasts of *Schizosaccharomyces japonicus* var. *versatilis*: a time-lapse microcinematographic study. *J. Gen. Microbiol.*, **130**, 625–630.

Garnjobst,L. and Tatum,E.L. (1967) A survey of new morphological mutants in *Neurospora crassa*. *Genetics*, **57**, 579–604.

Gimeno,C.J., Ljungdahl,P.O., Styles,C.A. and Fink,G.R. (1992) Unipolar cell divisions in the yeast *S.cerevisiae* lead to filamentous growth: regulation by starvation and RAS. *Cell*, **68**, 1077–1090.

Girbardt,M. (1979) A microfilamentous septal belt (FSB) during induction of cytokinesis in *Trametes versicolor* (L. ex Fr.). *Exp. Mycol.*, **3**, 215–228.

Gold,S., Duncan,G., Barrett,K. and Kronstad,J. (1994) cAMP regulates morphogenesis in the fungal pathogen *Ustilago maydis*. *Genes Dev.*, **8**, 2805–2816.

Gooday,G.W. (1971) An auxoradiographic study of hyphal growth of some fungi. *J. Gen. Microbiol.*, **67**, 125–133.

Gooday,G.W. and Trinci,A.P.J. (1980) Wall structure and biosynthesis in fungi. *Symp. Soc. Gen. Microbiol.*, **30**, 207–251.

Grove,S.N. and Bracker,C.E. (1970) Protoplasmic organization of hyphal tips among fungi: vesicles and Spitzenkörper. *J. Bacteriol.*, **104**, 989–1009.

Grove,S.N. and Sweigard,J.A. (1980) Cytochalasin A inhibits spore germination and hyphal tip growth in *Gilbertella persicaria*. *Exp. Mycol.*, **4**, 239–250.

Harding,R.W. and Melles,S. (1983) Genetic analysis of phototropism of *Neurospora crassa* perithecial beaks using white collar and albino mutants. *Plant Physiol.*, **72**, 996–1000.

Harold,F.M. (1990) To shape a cell: an inquiry into the causes of morphogenesis of microorganisms. *Microbiol. Rev.*, **54**, 381–431.

Harris,S.D., Morrell,J.L. and Hamer,J.E. (1994) Identification and characterization of *Aspergillus nidulans* mutants defective in cytokinesis. *Genetics*, **136**, 517–532.

Heath,I.B. (1990) The roles of actin in tip growth of fungi. *Int. Rev. Cytol.*, **123**, 95–127.

Howard,R.J. (1981) Ultrastructural analysis of hyphal tip cell growth in fungi: Spitzenkörper, cytoskeleton and endomembranes after freeze-substitution. *J. Cell Sci.*, **48**, 89–103.

Hunsley,D. and Gooday,G.W. (1974) The structure and development of septa in *Neurospora crassa*. *Protoplasma*, **82**, 125–146.

Johnson,T.E. (1976) Analysis of pattern formation in *Neurospora* perithecial development using genetic mosaics. *Dev. Biol.*, **54**, 23–36.

Kore-eda,S., Murayama,T. and Uno,I. (1991) Isolation and characterization of the adenylate cyclase structural gene of *Neurospora crassa*. *Jap. J. Genet.*, **66**, 317–334.

Lauter,F.R., Russo,V.E.A. and Yanofsky,C. (1992) Developmental and light regulation of *eas*, the structural gene for the rodlet protein of *Neurospora*. *Genes Dev.*, **6**, 2373–2381.

Maeda,H. and Ishida,N. (1967) Specificity of binding of hexopyranosyl polysaccharides with fluorescent brightener. *J. Biochem.*, **62**, 276–278.

Maheshwari,R. (1991) Microcycle conidiation and its genetic basis in *Neurospora crassa*. *J. Gen. Microbiol.*, **137**, 2103–2115.

McKerracher,L.J. and Heath,I.B. (1987) Cytoplasmic migration and intracellular organelle movements during tip growth of fungal hyphae. *Exp. Mycol.*, **11**, 79–100.

McLean,K.M. and Prosser,J.I. (1987) Development of vegetative mycelium during colony growth of *Neurospora crassa*. *Trans. Br. Mycol. Soc.*, **88**, 489–495.

Metzenberg,R.L., Stevens,J.N., Selker,E.U. and Morzycka-Wroblewska,E. (1985) Identification and chromosomal distribution of 5S rRNA genes in *Neurospora crassa*. *Proc. Natl Acad. Sci. USA*, **82**, 2067–2071.

Mitchell,T.K. and Dean,R.A. (1995) The cAMP-dependent protein kinase subunit is required for appressorium formation and pathogenesis by the rice blast pathogen *Magnaporthe grisea*. *Plant Cell*, **7**, 1869–1878.

Mitsuzawa,H. (1994) Increases in cell size at START caused by hyperactivation of the cAMP pathway in *Saccharomyces cerevisiae*. *Mol. Gen. Genet.*, **243**, 158–165.

Morris,N.R. (1976) Mitotic mutants of *Aspergillus nidulans*. *Genet. Res.*, **26**, 237–254.

Nurse,P. (1994) Fission yeast morphogenesis—posing the problems. *Mol. Biol. Cell*, **5**, 613–616.

Patton,A.M. and Marchant,R. (1978) An ultrastructural study of septal development in hyphae of *Polyporus biennis*. *Arch. Microbiol.*, **118**, 271–277.

Perkins,D.D., Radford,A., Newmeyer,D. and Björkman,M. (1982) Chromosomal loci of *Neurospora crassa*. *Microbiol. Rev.*, **46**, 426–570.

Raju,N.B. (1980) Meiosis and ascospore genesis in *Neurospora*. *Eur. J. Cell Biol.*, **23**, 208–233.

Read,N.D. (1983) A scanning electron microscopic study of the external features of perithecium development in *Sordaria humana*. *Can. J. Bot.*, **61**, 3217–3229.

Salo,V., Niini,S.S., Virtanen,I. and Raudaskoski,M. (1989) Comparative immunocytochemistry of the cytoskeleton in filamentous fungi with dikaryotic and multinucleate hyphae. *J. Cell Sci.*, **94**, 11–24.

Sambrook,J., Fritsch,E.H. and Maniatis,T. (1989) *Molecular Cloning: A Laboratory Manual*. Cold Spring Harbor Laboratory Press, Cold Spring Harbor, NY.

Sanger,F., Nicklen,S. and Coulson,A.R. (1977) DNA sequencing with chain-terminating inhibitors. *Proc. Natl Acad. Sci. USA*, **74**, 5463–5467.

Springer,M.L. and Yanofsky,C. (1989) A morphological and genetic analysis of conidiophore development in *Neurospora crassa*. *Genes Dev.*, **3**, 559–571.

Taylor,S.S., Buechler,J.A. and Yonemoto,W. (1990) cAMP-dependent protein kinase: framework for a diverse family of regulatory enzymes. *Annu. Rev. Biochem.*, **59**, 971–1005.

Terenzi,H.F., Flawia,M.M., Tellez-Inon,M. and Torres,H.N. (1976) Control of *Neurospora crassa* morphology by cyclic adenosine 3′, 5′-monophosphate and dibutyryl cyclic adenosine 3′, 5′-monophosphate. *J. Bacteriol.*, **126**, 91–99.

That,T.C.C., Rossier,C., Barja,F., Turian,G. and Roos,U. (1988) Induction of multiple germ tubes in *Neurospora crassa* by antitubulin agents. *Eur. J. Cell Biol.*, **46**, 68–79.

Tinsley,J.H., Minke,P.F., Bruno,K.S. and Plamann,M. (1996) p150Glued, the largest subunit of the dynactin complex, is nonessential in *Neurospora* but required for nuclear distribution. *Mol. Biol. Cell*, **7**, 731–742.

Toda,T., Cameron,S., Sass,P., Zoller,M., Scott,J.D., McMullen,B., Hurwitz,M., Krebs,E.G. and Wigler,M. (1987) Cloning and characterization of *BCY1*, a locus encoding a regulatory subunit of the cyclic AMP-dependent protein kinase in *Saccharomyces cerevisiae*. *Mol. Cell. Biol.*, **7**, 1371–1377.

Turian,G. and Bianchi,D.E. (1972) Conidiation in *Neurospora*. *Bot. Rev.*, **38**, 119–154.

Verde,F., Mata,J. and Nurse,P. (1995) Fission yeast cell morphogenesis: identification of new genes and analysis of their role during the cell cycle. *J. Cell Biol.*, **131**, 1529–1538.

Vollmer,S.J. and Yanofsky,C. (1986) Efficient cloning of genes of *Neurospora crassa*. *Proc. Natl Acad. Sci. USA*, **83**, 4869–4873.

Yarden,O., Plamann,M., Ebbole,D.J. and Yanofsky,C. (1992) *cot-1*, a gene required for hyphal elongation in *Neurospora crassa*, encodes a protein kinase. *EMBO J.*, **11**, 2159–2166.

Zoller,M., Kuret,J., Cameron,S., Levin,L. and Johnson,K.E. (1988) Purification and characterization of C1, the catalytic subunit of *Saccharomyces cerevisae* cAMP-dependent protein kinase encoded by *TPK1*. *J. Biol. Chem.*, **263**, 9142–9148.

Received on May 20, 1996; revised on July 10, 1996